

Quantifying Dermatochalasis Using 3-Dimensional Photogrammetry

Xueting Li¹ · Alexander C. Rokohl^{1,2} · Wanlin Fan¹ · Michael Simon^{1,2} ·
Xiaojun Ju¹ · Till Rosenkranz¹ · Philomena A. Wawer Matos^{1,2} · Yongwei Guo³ ·
Ludwig M. Heindl^{1,2}



Received: 2 July 2023 / Accepted: 20 October 2023 / Published online: 9 November 2023
© Springer Science+Business Media, LLC, part of Springer Nature and International Society of Aesthetic Plastic Surgery 2023

Abstract

Background Creating an appropriate treatment plan for patients with dermatochalasis requires careful investigation of the periocular region. Utilizing photographic documentation can assist physicians in conducting preoperative analysis and managing expectations regarding surgical outcomes.

Objectives This study aimed to quantify the periocular characteristics of dermatochalasis patients using standardized 3D imaging and to compare age and sex-related changes in periocular features.

Methods In this cross-sectional study, we recruited 145 Caucasian patients with periocular dermatochalasis, comprising 48 men and 97 women, aged between 35 and 91 years. Standardized three-dimensional facial photographs were taken using the 3D Imaging system VECTRA M3. Linear dimensions, curve length, angle, indices, and sizes were measured and analyzed, including palpebral fissure height (PFH), palpebral fissure width (PFW), upper lid

fold-palpebral margin distance (FPD), upper palpebral margin length (UPML), lower palpebral margin length (LPML), canthal tilt (CT), palpebral fissure index (PFI), upper eyelid area, and ocular surface area.

Results In the female group, the left-side PFH was slightly larger than the right-side PFH ($P = 0.023$), but the difference was less than 1mm. The corresponding PFI also showed a difference in the female group ($P = 0.009$). Statistically significant differences were shown in genders for specific parameters, except PFI ($P = 0.251$) and CT ($P = 0.098$). Among males, PFW ($R = -0.523$, $p < 0.001$) and LPML ($R = -0.514$, $P = 0.264$) decreased moderately with age. The correlation between UPML and age was weak ($R = -0.367$, $P = 0.010$). Similarly, among females, moderate correlations were found between age and PFW ($R = -0.566$, $P < 0.001$) and LPML ($R = -0.537$, $P < 0.001$). Additionally, PFH ($R = -0.315$, $P = 0.002$), UPML ($R = -0.381$, $P < 0.001$), and ocular surface area ($R = -0.457$, $P < 0.001$) showed weak correlations with age.

Conclusions The study found that dermatochalasis usually affects both eyes simultaneously, and age is a significant factor in the morphological changes of certain periocular features regardless of sex. The PFI is not influenced by age or sex. These findings may provide useful information for surgical planning and understanding age-related changes in the periocular area.

Level of Evidence V This journal requires that authors assign a level of evidence to each article. For a full description of these Evidence-Based Medicine ratings, please refer to the Table of Contents or the online Instructions to Authors www.springer.com/00266.

Keywords Dermatochalasis · Periocular morphology · Age · Anthropometry · Three-dimensional imaging

✉ Yongwei Guo
yongwei-guo@zju.edu.cn

✉ Ludwig M. Heindl
ludwig.heindl@uk-koeln.de

¹ Department of Ophthalmology, University of Cologne, Faculty of Medicine and University Hospital Cologne, Kerpener Straße 62, 50937 Cologne, Germany

² Center for Integrated Oncology (CIO), Aachen-Bonn-Cologne-Duesseldorf, Cologne, Germany

³ Eye Center, The Second Affiliated Hospital, School of Medicine, Zhejiang University, Zhejiang Provincial Key Laboratory of Ophthalmology, Zhejiang Provincial Clinical Research Center for Eye Diseases, Zhejiang Provincial Engineering Institute on Eye Diseases, Hangzhou, Zhejiang, China

Introduction

A person's appearance and how they are perceived affect social interactions. The periocular region, which is strongly associated with facial attractiveness, is particularly susceptible to showing signs of aging that are often considered less attractive. Dermatochalasis is an advanced form of skin aging that affects the periocular region, manifesting as laxity and thinning of the skin as well as atrophy of the periocular soft tissue that may result in anatomical misalignment and formation of rhytides. Colloquially referred to as “baggy eyes,” dermatochalasis is often considered a cosmetic problem that affects middle-aged and older individuals.

Blepharoplasty was developed to enhance the attractiveness of the periocular region and to achieve periocular rejuvenation [1]. Prior to performing surgery on patients with dermatochalasis, photographic documentation and careful, detailed evaluation of the patient's facial features are essential to create an appropriate treatment plan; any potential asymmetry should be identified and discussed with the patient. However, accurate evaluation of facial features can be challenging due to differences in photography sizes, head movements, and facial expressions.

To overcome these challenges, noninvasive 3D imaging technology that detects facial landmarks and measures a series of variables is used to record and analyze variations in the periocular region [2–6]. In previous studies, we found that the intrarater measurements exhibited the highest reliability, followed by the interrater and intramethod measurements [7]. These findings validated the method's reliability for 3D linear and areal measurements in the periocular region and identified the limitations in the reliability of volumetric measurements derived from direct measurements using a single image [4, 8]. Additionally, the pupil has been verified as the most stable landmark for establishing reference planes to describe periocular changes [9]. However, no 3D imaging technology-based studies have been conducted on patients with dermatochalasis. Therefore, our study aimed to analyze the periocular characteristics of patients with dermatochalasis before surgery and evaluate the impact of age and sex furtherly.

Methods

Participants and Recruitment

We recruited patients diagnosed with dermatochalasis between January 2022 and April 2023 at REDACTED. Each participant was of Caucasian ethnicity, aged over 18 years, and had no history of eyelid disease, trauma, or

surgery that could have impacted their facial morphology. Individuals with cognitive deficits or those who were unwilling or unable to cooperate were excluded. The study was conducted in accordance with the Declaration of Helsinki (as revised in 2013). The study was approved by the Ethics Committee of REDACTED (approval number: 17–199) and informed consent was taken from all individual participants.

Acquisition of Three-dimensional Facial Images

Stereophotography was performed using the VECTRA M3 3D Imaging System (Canfield Scientific, Inc., Parsippany, NJ, USA). The 3D camera was calibrated daily, and a trained operator (X.L.) captured all images following the manufacturer's guidelines. All images were captured in the same clinical photography room under standard ambient lighting without natural light sources. Patients were instructed to remove glasses, masks, and any other facial coverings, including facial makeup. Six cameras were located at a fixed distance and angle relative to the patient. Patients were seated in a fixed position and instructed to maintain neutral expression while looking directly into a mirror located in the upper middle region of the machine, keeping their eyes between the vertical and horizontal reference lines on the screen. Standard patient images were obtained, and all measurements and analyses were performed by the same operator (X. L.). Finally, proprietary image processing software Vectra® M3 (3D Imaging System; Canfield Scientific, Parsippany, NJ, USA) was used to measure and analyze the 3D facial models. A series of standardized landmarks in the periocular region was selected based on previously published studies [3, 4]. These landmarks are shown in frontal (Fig. 1A) and lateral (Fig. 1B) views, with their respective abbreviations defined in Table 1.

Additionally, we measured and calculated the palpebral fissure height (PFH), palpebral fissure width (PFW), upper lid fold-palpebral margin distance (FPD), curve length of the upper palpebral margin length (UPML), curve length of the lower palpebral margin length (LPML), angle of cantal tilt (CT), palpebral fissure index (PFI), upper eyelid surface area, and ocular surface area by clicking to connect the corresponding landmarks (Table 2).

Statistical Analysis

The Kolmogorov–Smirnov test for normality was used to evaluate the distribution of the data. Demographic and clinical characteristics are presented as mean \pm standard

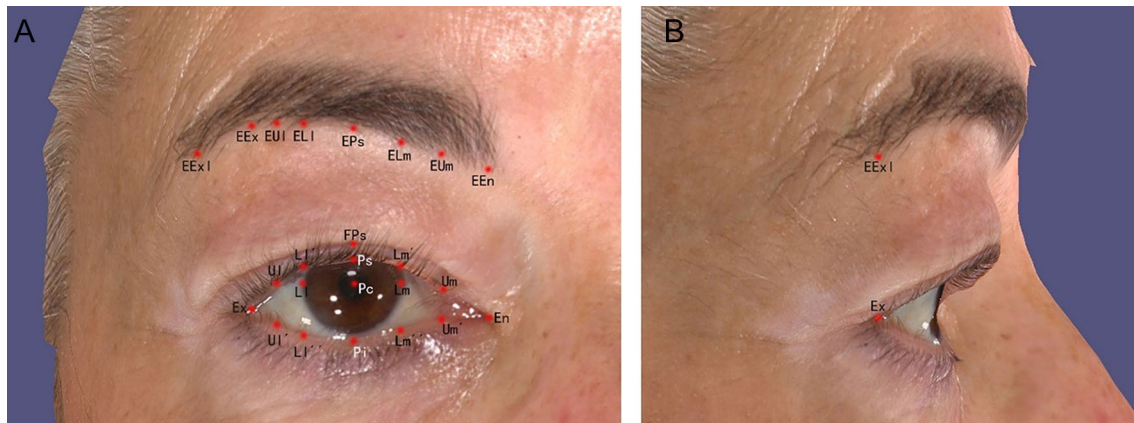


Fig. 1 The standardized landmarks of three-dimensional evaluation. **A** The frontal view of the periocular region; **B** The lateral view of the periocular region. Pc is the pupillary center. Lm and Ll are corneoscleral limbus point horizontal to Pc. Vertical to Pc are correspondent points, i.e., Eps, FPs, Ps, and Pi. Similarly, Elm, Lm', Lm'', are vertical to Lm, and ELl, Ll'', as well as Ll' are vertical to Ll. Um is the middle point between Endocanthion (En) and Lm', and Ul

is the middle point between Exocanthion (Ex) and Ll' at the upper palpebral margin on the lash roots. Likewise, Ul' and Um' are marked at the lower palpebral margin on the lash roots. Furthermore, EUm is vertical to Um, EEx is vertical to Ul, EEn is vertical to En, and EEx is also vertical to Ex at the inferior margin of eyebrows. EExI is vertical to Ex at the inferior margin of the eyebrow in the lateral review.

Table 1 Definition of abbreviations of periocular landmarks

Abbreviation of landmarks	Definition
En	Endocanthion, inner commissure of the palpebral fissure
Ex	Exocanthion, outer commissure of the lower and upper eyelash roots of the palpebral fissure
Pc	pupillary center
Ps	Palpebrae superioris, Point vertical to Pc at the upper palpebral margin on the lash roots
Pi	Palpebrae inferioris, Point vertical to Pc at the lower palpebral margin on the lash roots
FPs	Point vertical to Pc at the lid fold superioris
EPs	Point vertical to Pc at the inferior margin of eyebrows
Lm	Medial corneoscleral limbus point horizontal to pupillary center
Lm'	Point vertical to Lm at the upper palpebral margin on the lash roots
Lm''	Point vertical to Lm at the lower palpebral margin on the lash roots
Um	Middle point between En and Lm' at the upper palpebral margin on the lash roots
Um'	Middle point between En and Lm'' at the lower palpebral margin on the lash roots
Ll	Lateral corneoscleral limbus point horizontal to pupillary center
Ll'	Point vertical to Ll at the upper palpebral margin on the lash roots
Ll''	Point vertical to Ll at the lower palpebral margin on the lash roots
Ul	The middle between Ex and Ll' at the upper palpebral margin on the lash roots
Ul'	The middle between Ex and Ll'' at the lower palpebral margin on the lash roots
EEn	Point vertical to En at the inferior margin of eyebrows
EEx	Point vertical to Ex at the inferior margin of eyebrows
EExL	Point vertical to Ex at the inferior margin of eyebrow in the lateral review
EUm	Point vertical to Um at the inferior margin of eyebrows
ELm	Point vertical to Lm at the inferior margin of eyebrows
ELl	Point vertical to Ll at the inferior margin of eyebrows
EUI	Point vertical to Ul at the inferior margin of eyebrows

Adapted by permission from Springer Nature from Guo Y et al. Reliability of periocular anthropometry using three-dimensional digital stereophotogrammetry. *Graefes Arch Clin Exp Ophthalmol* 2019; 257:2517–31

Table 2 Definition of linear distance, curve, and size measurement variables for the periocular region

Abbreviation	Landmarks
Linear dimensions	
Palpebral fissure height, PFH	Ps-Pi
Palpebral fissure width, PFW	En-Ex
Upper lid fold-palpebral margin distance, FPD	Ps-FPs
Curve length	
Upper palpebral margin length, UPML	En-Um-Lm'-Ps-LI'-UI-Ex
Lower palpebral margin length, LPML	En-Um'-Lm''-Pi-LI''-UI'-Ex
Angle	
Canthal tilt, CT	Ex(l)-En(l)-En(r), or Ex(r)-En(r)-En(l)
Indices	
Palpebral fissure index, PFI	PFH/PFW
Sizes	
Upper eyelid area	EEEn-EUm-ELm-EPs-ELI-EUI-EEEx-EEExl-Ex-UI-LI'-Ps-Lm'-Um-En-EEEn
Ocular surface area	En-Um-Lm'-Ps-LI'-UI-Ex-UI'-LI''-Pi-Lm''-Um'-En

Adapted by permission from Springer Nature from Guo Y et al. Reliability of periocular anthropometry using three-dimensional digital stereophotogrammetry. *Graefes Arch ClinExp Ophthalmol* 2019; 257:2517–31

deviation (or median and interquartile intervals). Paired sample *t*-tests were conducted to compare bilateral eyes, and independent samples *t*-tests were performed for normally distributed data to compare different sexes. Wilcoxon signed-rank tests and Mann–Whitney U tests were employed for data that were not normally distributed. Pearson correlation coefficient was used for correlation analysis. The statistical analyses were conducted using SPSS software version 22 (IBM Corporation, Armonk, NY, USA). Figures were generated using GraphPad Prism 8.0.1 (GraphPad Software, San Diego, CA, USA). *P* values ≤ 0.05 were considered statistically significant.

Results

A total of 145 participants with dermatochalasis were enrolled in our study, ranging from 35 to 91 years of age (mean age of 59.120 ± 9.282 years). There were 290 eyes in 48 men (33.103%) and 97 women (66.897%).

Differences in Bilateral Periocular Area

Patients' right eyes were compared with their corresponding left eyes (Table 3). The PFH of the left eye was found to be greater than that of the right eye both in the total group and in the female group. Correspondingly, the PFI also differed significantly between the two sides, with the left eye showing higher values than the right eye in women.

However, the remaining parameters, including PFW, FPD as well as the curve length of UPML and LPML, CT angles, upper eyelid area, and ocular surface area did not show any difference between the two sides.

Differences Between Male and Female Patients

We also examined discrepancies between male (mean age of 61.420 ± 8.865 years) and female (mean age of 58.680 ± 9.362 years) patients (Table 4). There was no significant difference in patients' age according to sex; however, several characteristics differed significantly between the male group and the female group. Specifically, PFH and PFW measurements were significantly greater in the male group (9.680 ± 1.542 mm, 27.146 ± 2.689 mm, respectively) than in the female group (8.995 ± 1.494 mm, 25.884 ± 2.913 mm, respectively) (both $P < 0.001$). However, males had a shorter FPD (2.470 mm [3.658]) than females (3.051 mm [3.922]). Additionally, the male group had longer eyelids (UPML 35.830 ± 4.342 mm; LPML 29.762 ± 3.277 mm) than females (UPML 33.622 ± 4.417 mm; LPML 28.474 ± 3.246 mm). Moreover, the exposed ocular surface area in males was greater than that in females (2.069 ± 0.515 mm² and 1.895 ± 0.483 mm², respectively), and the male upper eyelid area (5.236 ± 1.179 mm²) was smaller than that of females (6.153 ± 1.382 mm²). However, there was no significant difference in CT and PFI between the sexes (all $P > 0.05$).

Table 3 Measurements difference between left and right eyes

Variable	Total (N = 145)			Male (n = 48)			Female (n = 97)					
	R	L	t value	P value	R	L	t value	P value	R	L	t value	P value
Linear dimensions(mm)												
PFH	9.086 ± 1.571	9.364 ± 1.505	-2.983	0.003*	9.582 ± 1.610	9.840 ± 1.470	-1.822	0.075	8.858 ± 1.518	9.111 ± 1.476	-2.304	0.023*
PFW	26.403 ± 2.836	26.212 ± 2.964	1.230	0.221	27.093 ± 2.902	27.199 ± 2.486	-0.337	0.708	26.023 ± 2.739	25.905 ± 2.787	0.752	0.454
FPD	2.973 (3.894)	2.967 (3.807)	-	0.128	2.759 (3.691)	1.622 (3.282)	-	0.155	2.896(3.884)	3.014(3.789)	-	0.396
Curve length (mm)												
UPML	34.539 ± 4.533	34.186 ± 4.894	1.597	0.113	36.022 ± 4.493	35.637 ± 4.224	1.162	0.251	33.790 ± 4.389	33.453 ± 4.462	1.166	0.246
LPML	28.904 ± 3.365	28.909 ± 3.260	-0.031	0.975	29.832 ± 3.365	29.693 ± 3.220	-0.438	0.663	28.435 ± 3.284	28.513 ± 3.224	-0.414	0.679
Angle (°)												
CT	170.763 ± 3.898	170.810 ± 4.298	-0.105	0.916	171.107 ± 4.214	171.593 ± 4.542	-0.615	0.542	170.590 ± 3.740	170.415 ± 4.138	0.324	0.747
Indices												
PFI	0.344 ± 0.051	0.356 ± 0.049	-3.060	0.003*	0.354 ± 0.054	0.362 ± 0.050	-1.129	0.102	0.341 ± 0.048	0.352 ± 0.049	-2.652	0.009*
Sizes (mm2)												
Upper eyelid area	5.815 ± 1.353	5.841 ± 1.338	-0.877	0.705	5.194 ± 1.137	5.279 ± 1.134	-0.743	0.461	6.123 ± 1.351	6.183 ± 1.418	-0.261	0.141
Ocular surface area	1.97165 ± 0.503	1.934 ± 0.498	1.129	0.232	2.097 ± 0.525	2.042 ± 0.509	0.990	0.327	1.910 ± 0.050	1.881 ± 0.486	0.029	0.450

R: Right eyes; L: Left eyes; PFH, Palpebral fissure height; PFW, Palpebral fissure width; FPD, Upper lid fold-palpebral margin distance; UPML, Upper palpebral margin length; LPML, Lower palpebral margin length; CT, Canthal tilt; PFI, Palpebral fissure index. Paired sample *t*-tests, except that FPD was analyzed by Wilcoxon signed-rank tests. **P* ≤ 0.05; ***P* ≤ 0.001

Table 4 Variable measurement differences between different gender

Variable	M	F	P
Linear dimensions			
PFH	9.680 ± 1.542	8.995 ± 1.494	< 0.001**
PFW	27.146 ± 2.689	25.884 ± 2.913	< 0.001**
FPD	2.470 (3.658)	3.051 (3.922)	0.016*
Curve length			
UPML	35.830 ± 4.342	33.622 ± 4.417	< 0.001**
LPML	29.762 ± 3.277	28.474 ± 3.246	0.002*
Angle			
CT	171.350 ± 4.365	170.502 ± 3.934	0.098
Indices			
PFI	0.358 ± 0.053	0.349 ± 0.059	0.251
Sizes			
Upper eyelid area	5.236 ± 1.179	6.153 ± 1.382	< 0.001**
Ocular surface area	2.069 ± 0.515	1.895 ± 0.483	0.005*

M, male; F, female; PFH, Palpebral fissure height; PFW, Palpebral fissure width; FPD, Upper lid fold-palpebral margin distance; UPML, Upper palpebral margin length; LPML, Lower palpebral margin length; CT, Canthal tilt; PFI, Palpebral fissure index. Independent samples *t*-test, except that FPD was analyzed by Mann–Whitney U test. * $P \leq 0.05$; ** $P \leq 0.001$

Correlation Between Age and Periocular Parameters

In the male group, PFW ($R = -0.523$, $P < 0.001$) and LPML ($R = -0.514$, $P = 0.264$) were moderately correlated with age, whereas the correlation between UPML and age was weak ($R = -0.367$, $P = 0.010$) (Fig. 2). Similarly, in the female group, a moderate correlation was observed between age and PFW ($R = -0.566$, $P < 0.001$) as well as age and LPML ($R = -0.537$, $P < 0.001$). Furthermore, PFH ($R = -0.315$, $P = 0.002$), UPML ($R = -0.381$, $P < 0.001$), and ocular surface area ($R = -0.457$, $P < 0.001$) showed a weak correlation with age of female (Fig. 3).

Discussion

Conventionally the direct anthropometry and 2D systems are standard methods for eyelids and brows related parameters measuring [10]. Direct anthropometry, which uses sliding and spreading calipers, is time-consuming and requires patient cooperation, while the 2D system, which allows for indirect anthropometry, requires labeling facial landmarks, attaching a ruler to the patient's face as a reference, and capturing images with different gazes [11]. Facial imaging contains more feature information of patients with dermatochalasis. Over the last decade, 3D imaging has become an area of interest in facial imaging, gradually replacing 2D systems and traditional anthropometry. Several studies have been devoted to the reliability, reproducibility, and accuracy

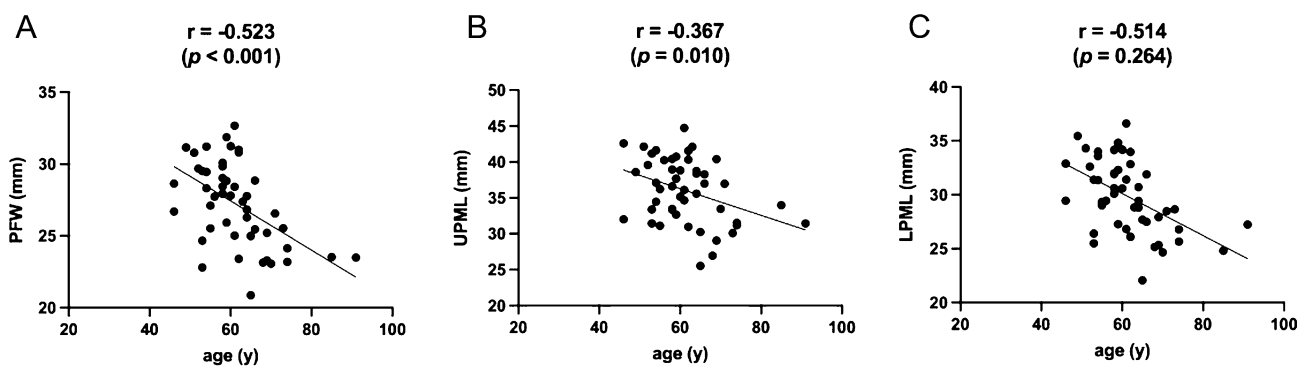


Fig. 2 Correlations between the periocular variables and age in males. **A** The correlation between palpebral fissure width (PFW) and age (Pearson's correlation coefficient = -0.523). **B** The correlation between upper palpebral margin length (UPML) and age (Pearson's

correlation coefficient = -0.367). **C** The correlation between lower palpebral margin length (LPML) and age (Pearson's correlation coefficient = -0.514).

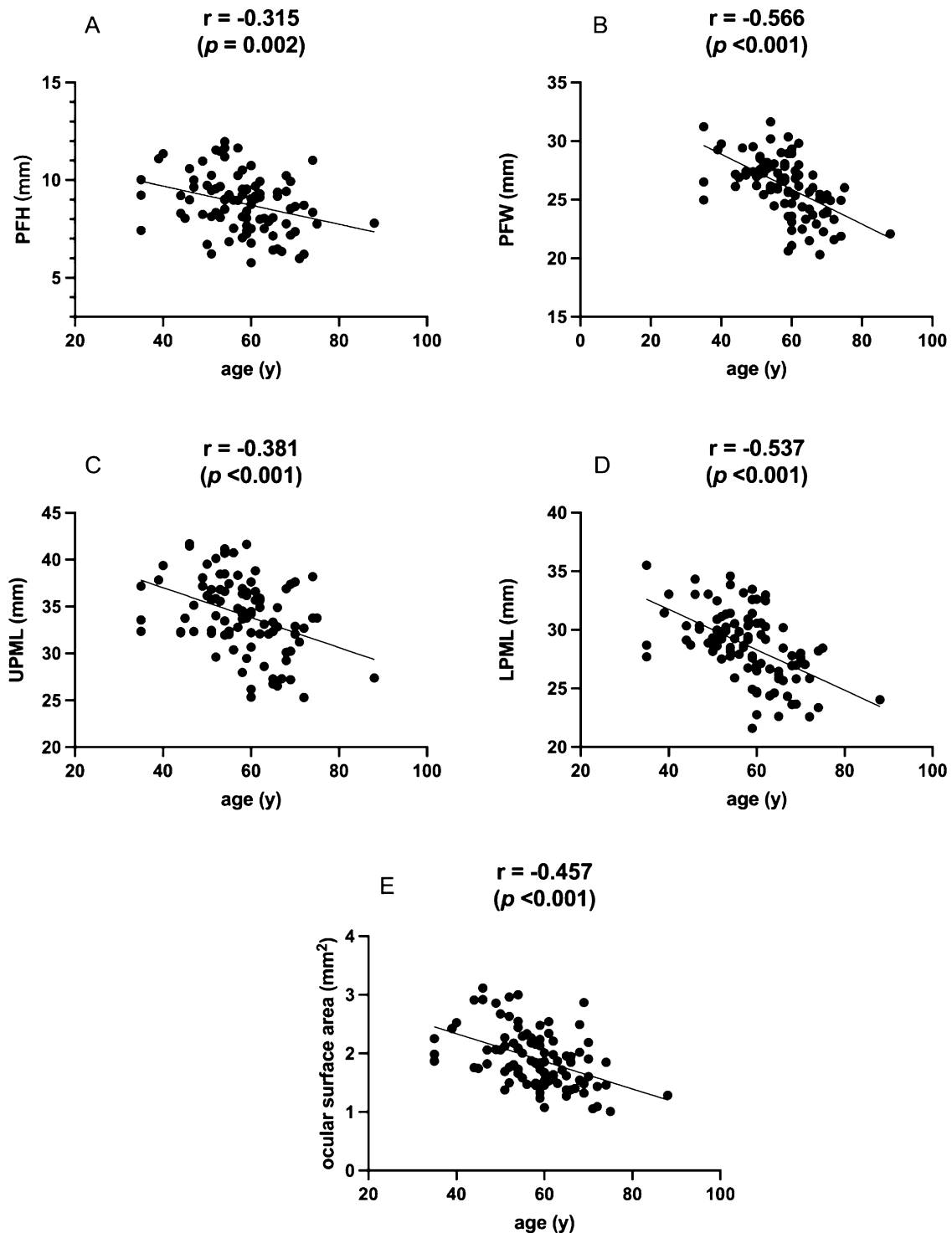


Fig. 3 The correlation between the periocular variables and age in females. **A** The correlation between palpebral fissure height (PFH) and age (Pearson's correlation coefficient = -0.315). **B** The correlation between palpebral fissure width (PFW) and age (Pearson's correlation coefficient = -0.566). **C** The correlation between upper

palpebral margin length (UPML) and age (Pearson's correlation coefficient = -0.381). **D** The correlation between lower palpebral margin length (LPML) and age (Pearson's correlation coefficient = -0.537). **E** The correlation between ocular surface area and age (Pearson's correlation coefficient = -0.457).

of 3D photogrammetry in soft tissue evaluation [12–15], 3D stereophotogrammetry seems to be an optimal and accurate tool, especially for measuring the depth of facial sculptures [16, 17] and representing the texture and color of skin [15, 18]. Additionally, 3D imaging methods can provide measurements of linear distance, angle, size, and volume, as well as a permanent record of consultations [19]. In this study, we used the 3D stereophotogrammetry to analyze bilateral periocular regions of patients with dermatochalasis and evaluated age-dependent changes, the factors strongly associated with PFW and LPML are demonstrated.

Left–right bilateral symmetry is considered as an important aspect of creating beauty. Our study showed that PFH was more extensive on the left side than on the right side. As there was no significant difference in PFW, PFI was also greater on the left side. Except for PFH and PFI, no significant differences were noted in other parameters such as FPD, UPML and LPML, CT angles, upper eyelid area, and ocular surface area. The prevalence of asymmetry varies according to measurement criteria. In our study, the difference in PFH between the left and right sides was less than 1 mm, consistent with previously described differences in perceived asymmetry [20, 21]. Our findings also align with the work by Pool et al., which used 2D photo-assisted analysis and found no significant difference in the mean eyelid fissure height between the right and left eyes [22]. Our observations verified that patients with dermatochalasis exhibit bilateral symmetry in the periocular area.

Our study identified statistically significant sex-based differences in the manifestation of dermatochalasis. Specifically, we found that females had narrower PFH and PFW, longer FPD, shorter eyelid length, larger upper eyelid area, and smaller ocular surface area than males. These differences may be attributed to sex-based variations in tarsal plate size and axial ocular globe projection [23]. Our findings are consistent with those reported in other racial and ethnic groups, e.g., narrower PFW has also been documented in South Indian and Chinese females [24–26]. These differences highlight the importance of considering sex-related variances in upper eyelid morphology during blepharoplasty. Women generally have a larger upper eyelid area and a longer double eyelid fold than men, resulting in relatively smaller PFH and ocular surface area. Therefore, caution is necessary when removing excess skin; the amount might be less than that for men to avoid creating an excessively large PFH and ocular surface area, which could lead to an unnatural or “operated” appearance.

Age is widely recognized as the primary risk factor for sagging eyelids, as skin redundancy increases with age, leading to protrusion or drooping of the upper eyelids below the eyelashes [27–29]. Both genetic factors and extrinsic mechanisms such as chronic sunlight exposure,

alcohol consumption, smoking, and nutritional deficiencies have been reported to influence skin aging [30]. The facial skeleton provides the structural framework for the overlying soft tissues. Notably, the process of facial skeleton resorption in the periorbital region, specifically involving the superomedial and inferolateral aspects of the orbit [31], leads to the movement of the location of the attachments of facial ligaments and muscles through the periosteum [32]. With advancing age, women experience an increase in both bony orbital volume and anterior globe position, while these measurements remain stable in men [33]. Muscular imbalance, loss of supportive structure volume, and drooping of the upper and midfacial feature could contribute to age-related changes in the periorbital region. In previous studies, sagging of eyelids was assessed using a 4-level Photonumerical Severity Scale, which classified the severity of sagging based on the relative position of the upper eyelid skin and the eyelashes [34]. Our study instead used a quantitative approach to present the severity of dermatochalasis by measuring periocular parameters. Our findings indicated that PFW and LPML were particularly susceptible to the effects of aging in both men and women. Moreover, UPML was noted to decrease slightly with age in the male group, and slight reductions of PFH, UPML, and ocular surface area occurred with age in the female group.

The PFW decreases in older individuals, likely due to increased skin laxity at the lateral and medial canthal tendon, causing a narrowing of the palpebral fissure. The minimal change in PFH is attributed to slightly weaker skin laxity in the central area compared to the periphery. When comparing between different ethnic populations, we found that reduced PFW was also documented in Korean and Turkish females: Kwon et al. [35] reported that Korean females over 60 years of age had the smallest PFH and PFW compared with younger or middle-aged females, and Direk et al. [36] found that Turkish females over 60 years of age had shorter PFH and narrower PFW compared with younger and middle-aged females. However, these studies did not include male participants. Additionally, these associations were only shown for the age group as a whole; a linear relationship with age was not demonstrated. Similarly, Raschke et al. [37] studied age-related anthropometric changes in Caucasians, but their findings were restricted to the perioral region. Park et al. demonstrated age-dependent shrinkage of the exposed corneal surface; however, their method involved qualitative analysis of 2D digital pictures and relied on the assumption that the pupil in each image was perfectly round. Moreover, PFH remains relatively stable with age, while LPML undergoes significant changes, indicating the laxity of the lower eyelid skin and the medial and lateral canthal tendons over time. This leads to a tendency for more ectropion rather than ptosis.

Based on our findings, strategic planning for operations should consider customized age and gender-specific techniques for blepharoplasty to preserve a natural and age-appropriate appearance.

In the preoperative phase of eyelid plastic surgery, in addition to comprehensive medical history evaluation and clinical examination, surgeons usually perform preoperative photography. This process involves identifying redundant upper eyelid skin, documenting any asymmetries, and so on. Our study emphasizes the importance of paying sufficient attention to the eye contour, especially in elderly patients with dermatochalasis. Regardless of gender, older patients should undergo a thorough assessment of eyelid laxity before surgery, which may include tests like the snap-back and pull-away tests. Especially the patients with eyelid skin laxity, it is essential to consider the condition of their inner and outer canthal ligaments. The decision to perform lateral canthopexy should be carefully considered, potentially addressing all symptoms in one surgery. During blepharoplasty, special attention should be given to the skin near the lateral canthus, and the amount of resection may need adjustment. Furthermore, as patients age, it becomes increasingly crucial to focus on postoperative complications, particularly lower eyelid malposition.

In our study, there are certain limitations that need to be acknowledged. Some studies define the upper eyelid not by the inferior margin of the brow but by the superior orbital rim [38]. However, in the case of the photograph, identifying the orbital rim beneath superficial tissue may lead to inaccuracies, especially in patients with dermatochalasis. Moreover, our objective is to measure the entire upper eyelid, and it is evident that demarcating below the orbital rim only represents a portion of the upper eyelid. But some patient's eyebrow shape contour may be not very clear. To enhance precision and reduce inter-patient variability, we have standardized the area measurement by incorporating eight points along the inferior margin of the eyebrow for each patient. This approach aims to minimize errors and variations among patients as effectively as possible. Additionally, it is important to note an imbalance in the gender distribution of our participants, with more females than males. This disparity may be due to increased concern about appearance and a higher willingness among women to undergo blepharoplasty compared to men. Furthermore, our study focused solely on pre-surgery patients and their characteristics; post-surgery data were not included in the current study. Finally, this paper solely examines the Caucasian ethnicity, which entails certain racial limitations, and suggests the need for future research involving a broader range of ethnic groups. These factors should be taken into consideration when interpreting our results.

In future investigations, we aspire to address these limitations by including a more balanced representation of male participants. Additionally, we intend to delve deeper into the post-surgery changes following blepharoplasty, employing 3D imaging for a comprehensive analysis in different races.

Conclusions

Our study of periocular characteristics in patients with dermatochalasis found that bilateral changes tended to appear simultaneously. Age was found to significantly affect certain periocular morphological changes, particularly the PFW and LPML. PFI did not appear to be influenced by age or sex. Our study provides ophthalmologists with valuable resources to improve understanding of morphology associated with dermatochalasis, develop anti-aging cosmetic surgery plans, and evaluating postoperative results.

Funding This study was supported by the State Scholarship Fund from China Scholarship Council (Nr. 202006370027 to X.L.), and the National Natural Science Foundation of China (Nr. 82102346 to Y.G.).

Declarations

Conflict of interest The authors declared no potential conflicts of interest with respect to the research, authorship, and publication of this article.

Ethical Approval All procedures performed in studies involving human participants were in accordance with the Declaration of Helsinki (as revised in 2013). The study was approved by the Ethics Committee of REDACTED (approval number: 17–199).

Informed Consent Informed consent was taken from all individual participants.

References

1. Espinoza GM, Holds JB (2005) Evolution of eyelid surgery. *Facial Plast Surg Clin N Am* 13(4):505–510
2. Guo Y et al (2020) A simple standardized three-dimensional anthropometry for the periocular region in a European population. *Plast Reconstr Surg* 145(3):514e–523e
3. Guo Y et al (2021) A novel approach quantifying the periorbital morphology: a comparison of direct, 2-dimensional, and 3-dimensional technologies. *J Plast Reconstr Aesthet Surg* 74(8):1888–1899
4. Guo Y et al (2019) Reliability of periocular anthropometry using three-dimensional digital stereophotogrammetry. *Graefes Arch Clin Exp Ophthalmol* 257(11):2517–2531
5. Hou X et al (2021) A novel standardized distraction test to evaluate lower eyelid tension using three-dimensional

- stereophotogrammetry. *Quant Imaging Med Surg* 11(8):3735–3748
6. Hou XY et al (2022) A modified 3D stereophotogrammetry-based distraction test for assessing lower eyelid tension. *Int J Ophthalmol* 15(11):1757–1764
 7. Liu J et al (2021) Reliability of stereophotogrammetry for area measurement in the periocular region. *Aesthet Plast Surg* 45(4):1601–1610
 8. Guo Y et al (2023) A novel standardized approach for the 3D evaluation of upper eyelid area and volume. *Quant Imaging Med Surg* 13(3):1686–1698
 9. Liu J et al (2023) Age-related changes of the periocular morphology: a two- and three-dimensional anthropometry study in Caucasians. *Graefes Arch Clin Exp Ophthalmol* 261(1):213–222
 10. Macdonald KI et al (2014) Eyelid and brow asymmetry in patients evaluated for upper lid blepharoplasty. *J Otolaryngol Head Neck Surg* 43(1):36
 11. Kashkouli MB et al (2017) Periorbital facial rejuvenation; applied anatomy and pre-operative assessment. *J Curr Ophthalmol* 29(3):154–168
 12. Dindaroğlu F et al (2016) Accuracy and reliability of 3D stereophotogrammetry: a comparison to direct anthropometry and 2D photogrammetry. *Angle Orthod* 86(3):487–494
 13. Liu J et al (2021) Accuracy of 3-dimensional stereophotogrammetry: comparison of the 3dMD and Bellus3D facial scanning systems with one another and with direct anthropometry. *Am J Orthod Dentofac Orthop* 160(6):862–871
 14. Mao B et al (2022) The accuracy of a three-dimensional face model reconstructing method based on conventional clinical two-dimensional photos. *BMC Oral Health* 22(1):413
 15. Savoldelli C et al (2019) Accuracy, repeatability and reproducibility of a handheld three-dimensional facial imaging device: the Vectra H1. *J Stomatol Oral Maxillofac Surg* 120(4):289–296
 16. Anas IY, Bamgbose BO, Nuhu S (2019) A comparison between 2D and 3D methods of quantifying facial morphology. *Heliyon* 5(6):e01880
 17. Ueda N et al (2021) Assessment of facial symmetry by three-dimensional stereophotogrammetry after mandibular reconstruction: a comparison with subjective assessment. *J Stomatol Oral Maxillofac Surg* 122(1):56–61
 18. Ding Y et al (2015) Combination of 3D skin surface texture features and 2D ABCD features for improved melanoma diagnosis. *Med Biol Eng Comput* 53(10):961–974
 19. Meng T et al (2020) Identifying facial features and predicting patients of acromegaly using three-dimensional imaging techniques and machine learning. *Front Endocrinol (Lausanne)* 11:492
 20. Song WC et al (2007) Asymmetry of the palpebral fissure and upper eyelid crease in Koreans. *J Plast Reconstr Aesthet Surg* 60(3):251–255
 21. Karlin JN, Rootman DB (2020) Brow height asymmetry before and after eyelid ptosis surgery. *J Plast Reconstr Aesthet Surg* 73(2):357–362
 22. Pool SM, van der Lei B (2015) Asymmetry in upper blepharoplasty: a retrospective evaluation study of 365 bilateral upper blepharoplasties conducted between January 2004 and December 2013. *J Plast Reconstr Aesthet Surg* 68(4):464–468
 23. Bashour M, Harvey J (2000) Causes of involuntal ectropion and entropion-age-related tarsal changes are the key. *Ophthalmic Plast Reconstr Surg* 16(2):131–141
 24. Vasanthakumar P, Kumar P, Rao M (2013) Anthropometric analysis of palpebral fissure dimensions and its position in South Indian ethnic adults. *Oman Med J* 28(1):26–32
 25. Wu XS et al (2010) Investigation of anthropometric measurements of anatomic structures of orbital soft tissue in 102 Young Han Chinese adults. *Ophthalmic Plast Reconstr Surg* 26(5):339–343
 26. Li Q et al (2016) Normative anthropometric analysis and aesthetic indication of the ocular region for young Chinese adults. *Graefes Arch Clin Exp Ophthalmol* 254(1):189–197
 27. Flament F et al (2020) Age-related changes to characteristics of the human eyes in women from six different ethnicities. *Skin Res Technol* 26(4):520–528
 28. Sforza C et al (2009) Age- and sex-related changes in the soft tissues of the orbital region. *Forensic Sci Int* 185(1–3):115.e1–115.e8
 29. Liu Y et al (2013) A 3-dimensional anthropometric evaluation of facial morphology among Chinese and Greek population. *J Craniofac Surg* 24(4):e353–e358
 30. Guinot C et al (2002) Relative contribution of intrinsic vs extrinsic factors to skin aging as determined by a validated skin age score. *Arch Dermatol* 138(11):1454–1460
 31. Kahn DM, Shaw RB Jr (2008) Aging of the bony orbit: a three-dimensional computed tomographic study. *Aesthet Surg J* 28(3):258–264
 32. Mendelson B, Wong CH (2020) Changes in the facial skeleton with aging: implications and clinical applications in facial rejuvenation. *Aesthet Plast Surg* 44(4):1151–1158
 33. Ugradar S et al (2022) Orbital aging: a computed tomography-based study of 240 orbits. *Plast Reconstr Surg* 150(3):536e–545e
 34. Jacobs LC et al (2014) Intrinsic and extrinsic risk factors for sagging eyelids. *JAMA Dermatol* 150(8):836–843
 35. Kwon SH et al (2021) Three-dimensional photogrammetric study on age-related facial characteristics in Korean females. *Ann Dermatol* 33(1):52–60
 36. Direk FK et al (2016) Anthropometric analysis of orbital region and age-related changes in adult women. *J Craniofac Surg* 27(6):1579–1582
 37. Raschke GF et al (2014) Perioral aging—an anthropometric appraisal. *J Craniofac Surg* 42(5):e312–e317
 38. Hyer JN et al (2021) Validating three-dimensional imaging for volumetric assessment of periorbital soft tissue. *Orbit* 40(1):9–17

Publisher's Note Springer Nature remains neutral with regard to jurisdictional claims in published maps and institutional affiliations.

Springer Nature or its licensor (e.g. a society or other partner) holds exclusive rights to this article under a publishing agreement with the author(s) or other rightsholder(s); author self-archiving of the accepted manuscript version of this article is solely governed by the terms of such publishing agreement and applicable law.